Applied Surface Science 257 (2011) 5581–5585

Contents lists available at ScienceDirect

Applied Surface Science

journal homepage: www.elsevier.com/locate/apsusc

Corrosion properties of aluminium coatings deposited on sintered NdFeB by ion-beam-assisted deposition

Shoudong Mao, Hengxiu Yang, Jinlong Li, Feng Huang, Zhenlun Song*

Ningbo Institute of Materials Technology and Engineering, Chinese Academy of Sciences, 519 Zhuangshi Road, Ningbo 315201, China

ARTICLE INFO

Article history:
Received 25 December 2010
Received in revised form 11 January 2011
Accepted 11 January 2011
Available online 2 February 2011

Keywords:
NdFeB
Aluminium coatings
Magnetron sputtering
IBAD
Corrosion resistance

ABSTRACT

Pure Al coatings were deposited by direct current (DC) magnetron sputtering to protect sintered NdFeB magnets. The effects of Ar^+ ion-beam-assisted deposition (IBAD) on the structure and the corrosion behaviour of Al coatings were investigated. The Al coating prepared by DC magnetron sputtering with IBAD (IBAD-Al-coating) had fewer voids than the coating without IBAD (Al-coating). The corrosion behaviour of the Al-coated NdFeB specimens was investigated by potentiodynamic polarisation, a neutral salt spray (NSS) test, and electrochemical impedance spectroscopy (EIS). The pitting corrosion of the Al coatings always began at the voids of the grain boundaries. Bombardment by the Ar^+ ion-beams effectively improved the corrosion resistance of the IBAD-Al-coating.

1. Introduction

Since 1984, sintered NdFeB magnets have been widely used for their excellent magnetic properties [1]. However, their poor corrosion resistance in various environments hinders their further application [2–6]. Their poor corrosion resistance is due to the existence of multiple phases in the microstructure. The sintered NdFeB magnets are composed of three basic phases: the matrix phase, which is the ferromagnetic tetragonal compound $Nd_2Fe_{14}B$, the Nd-rich phase Nd_4Fe, and the B-rich phase $Nd_{1+\varepsilon}Fe_4B_4$. Galvanic corrosion easily happens between the electrochemically highly active Nd-rich phase and the matrix phase [5].

Many attempts have been made to improve the corrosion resistance of the sintered NdFeB magnets, including alloy additions [7–9] and surface coatings [10–14]. In industry, electroplating is a widely used method with good performance and low processing costs [10,11]. Meanwhile, physical vapour deposition (PVD) methods, such as evaporation and sputtering, are becoming competitive alternatives to electroplating. Aluminium (Al) is well suited to provide corrosion protection for its low cost and high corrosion resistance [15,16]. In industry, Al coatings deposited by evaporation [13] or ion vapour deposition (IVD) [14] have been applied for the protection of NdFeB. However, because of the low kinetic energies of evaporant atoms (approximately 0.1 eV) [17], the coatings prepared by evaporation and IVD always present a columnar structure with a high concentration of inter-column defects (such as voids and micropores). These defects could result in premature failure of the coatings [18,19]. After deposition, a heat treatment may be necessary to improve the poor adhesion between the evaporated Al coating and the magnet [20]. However, the high temperatures often cannot be tolerated by the sintered NdFeB. Because the kinetic energy of sputtered atoms (typically 1–10 eV) is higher than that of the evaporated atoms, the adhesion and the porosity of the sputtered coatings can be improved [17,21]. However, according to our previous works, the sputtered Al coatings still presented columnar structures [22].

The porosity and the columnar structure in the evaporated and sputtered coatings can be overcome by simultaneous ion bombardment during deposition, which can provide additional energies to the depositing atoms. Several works on the corrosion protection of ion-beam-assisted deposition (IBAD) coatings show that the IBAD coatings have a lower porosity than the evaporated or sputtered coatings [16,23–25]. However, the application of IBAD coatings on sintered NdFeB magnets is lacking. The corrosion process of the IBAD coatings on the sintered NdFeB magnets is also seldom studied.

In this work, IBAD-Al-coating was deposited on sintered NdFeB. The effects of Ar^+ ion-beams on the structure of the coating were investigated. The correlation between the porosity and the pitting corrosion of the coatings was also studied.

2. Experimental details

Sintered NdFeB specimens (banded 35 H, Yunshen Co. Ltd, in a demagnetised state) with a size of

* Corresponding author. Tel.: +86 574 87911131; fax: +86 574 86685159.
E-mail address: songzhenlun@nimte.ac.cn (Z. Song).

0169-4332/$ – see front matter © 2011 Elsevier B.V. All rights reserved.
doi:10.1016/j.apsusc.2011.01.049

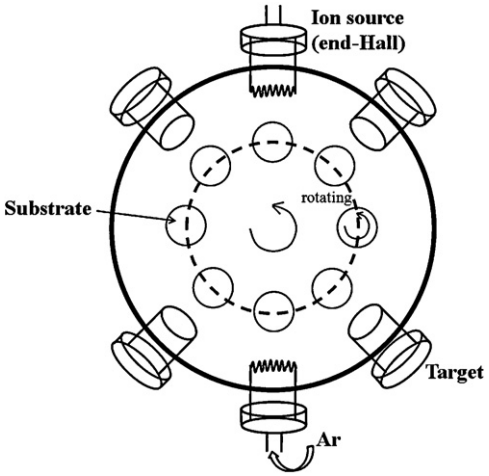

Fig. 1. Schematic of the magnetron sputtering apparatus designed to apply protective coatings to magnets [26].

20 mm × 10 mm × 5 mm were grounded, polished to a mirror surface and then, ultrasonically cleaned in acetone followed by alcohol.

Deposition was carried out in a magnetron sputtering apparatus designed to apply protective coatings to magnets. A schematic of the apparatus is shown in Fig. 1. The chamber was evacuated to a base pressure of 5×10^{-4} Pa. Pure Ar (99.999%) was introduced at a constant flow rate of 40 sccm to achieve the desired sputtering pressure of 0.5 Pa. Before deposition, the specimens were cleaned using Ar^+ ion beams, which were provided by two end-Hall ion guns, for 10 min. The IBAD-Al-coating was prepared by direct current (DC) magnetron sputtering from four Al targets (99.999%). Simultaneously, Ar^+ ion beam bombardment was applied by the two end-Hall ion guns, which had an energy of 150 V × 1 A. The angle of incidence was 30° from the substrate normal. In addition, Al-coating without additional bombardment was deposited by DC magnetron sputtering as a reference. Both the Al-coating and the IBAD-Al-coating were deposited at room temperature.

The thickness of the coatings was measured by a surface profilometer (Alpha-Step, IQ) employing a step formed by a shadow mask. The thickness of the Al-coating and the IBAD-Al-coating were approximately 5 μm. The micrographs of the specimens were observed by a scanning electron microscope (SEM, S-4800, Hitachi). X-ray photoelectron spectrometry (XPS, Axis Ultra DLD, Kratos) was applied to analyse the chemical state of the oxide films on the coatings. The corrosion behaviour was investigated by potentiodynamic polarisation and electrochemical impedance spectroscopy (EIS) in a 3.5 wt.% NaCl solution at 25 ± 3 °C. A conventional three-electrode cell was used with an Ag/AgCl electrode (saturated KCl) as the reference electrode, and a platinum sheet (20 mm × 10 mm) was used as the auxiliary electrode. The exposed surface of the working electrodes was 1 cm^2. To allow time for the stationary potential to stabilise, all systems were kept in solutions for 1 h before measurement. The potentiodynamic polarisation experiments were performed on a potentiostat/galvanostat (Autolab, Ecochimie). The EIS tests were performed using another piece of electrochemical equipment (273A, Princeton). A neutral salt spray (NSS) test was also performed to investigate the corrosion resistance of the specimens using a standard salt spray cabinet spraying NaCl solution (50 g/dm^3) at 35 ± 2 °C. The evolution of the corrosion phenomena was visually observed up to 10 day.

3. Results and discussion

3.1. Characteristics of the coatings

The SEM surface micrographs of the Al-coating shown in Fig. 2a and b reveal the presence of various grain sizes. A number of voids were distributed at the grain boundaries. The cross-sectional micrograph of the Al-coating shown in Fig. 2c presents evidence of a columnar structure. However, there are much fewer voids distributed at the grain boundaries of the IBAD-Al-coating, indicating low porosity (Fig. 2d and e). Meanwhile, as shown in Fig. 2f, the columnar structure, which can be seen in the Al-coating, is less visible in the IBAD-Al-coating. The cross-sectional micrographs also show that the Al-coating and the IBAD-Al-coating were well adhered to the substrate and that they did not develop cracks.

The columnar structure in the Al-coating is susceptible to a high density of defects during growth. During the growth of the IBAD-Al-coating, the bombardment of Ar^+ ions can enhance the nucleation rate and the adatom mobility, which can result in the removal of voids and disruption of the columnar growth. The two improvements may account for the densification of the IBAD-Al-coating at a low deposition temperature [27].

3.2. Corrosion resistance

Fig. 3 shows the potentiodynamic polarisation curves of three different specimens: (a) sintered NdFeB coated with Al (Al/NdFeB), (b) sintered NdFeB coated with IBAD-Al (IBAD-Al/NdFeB), and (c) bare sintered NdFeB. The bare sintered NdFeB exhibits an actively dissolving behaviour in the anodic region. Both the Al/NdFeB and the IBAD-Al/NdFeB first exhibit a passive-like anodic behaviour and then, switch to an actively dissolving behaviour as the potential increases. The passive-like anodic behaviour would be caused by the formation of oxide films on the Al coatings in the electrolyte. The corrosion current densities i_{corr} were calculated by GPES software near zero overall current. The i_{corr} of the Al/NdFeB (0.091 μA cm^2) and the IBAD-Al/NdFeB (0.023 μA cm^2) were approximately two orders of magnitude smaller than that of the bare sintered NdFeB (4.6 μA cm^2). This indicates that both the Al-coating and IBAD-Al-coating can effectively improve the corrosion resistance of the sintered NdFeB. The lower i_{corr} of the IBAD-Al/NdFeB indicates that it has better corrosion resistance than the Al/NdFeB.

The optical photographs of the Al/NdFeB and the IBAD-Al/NdFeB specimens after the 10-day NSS test are shown in Fig. 4. The Al/NdFeB is completely covered by the rusty corrosion products (Fig. 4a). However, there are only some rusty corrosion products distributed on the edge of the IBAD-Al/NdFeB (Fig. 4b). Therefore, the IBAD-Al/NdFeB has better corrosion resistance than the Al/NdFeB in the NSS test. This result is consistent with the potentiodynamic polarisation results.

3.3. Oxide films on coatings

Fig. 5 illustrates the XPS high-resolution spectra of the Al/NdFeB and IBAD-Al/NdFeB systems after 1 h of immersion in a 3.5 wt.% NaCl solution. The chemical states of the oxide films on the Al/NdFeB and the IBAD-Al/NdFeB are similar. The Al 2p spectrum is shown in Fig. 5a; the two peaks represent the metal and the oxide states, respectively. The binding energies of Al^{metal} and Al^{3+} are 72.9 eV and 75.3 eV, respectively. The O 1s spectrum is shown in Fig. 5b, which should be contributed by OH^- at 532.2 eV. Therefore, the oxide films on the Al-coating and the IBAD-Al-coating should be in the $Al(OH)_3$ state. The formation of the oxide films on the Al-coating and the IBAD-Al-coating in a NaCl solution can be expressed